

The strengthening effect of polystyrene foam filling in aluminum thin-walled cylindrical tubes

A.K. Toksoy^a, M. Güden^{a,b,*}

^aDepartment of Mechanical Engineering, Izmir Institute of Technology, Gülbahçe Köyü, Urla, Izmir, Turkey

^bCenter for Materials Research, Izmir Institute of Technology, Gülbahçe Köyü, Urla, Izmir, Turkey

Received 19 September 2003; accepted 26 July 2004

Abstract

The strengthening effect of foam filling in thin-walled circular tubes, deforming in diamond and concertina modes, was investigated in polystyrene foam filled aluminum tubes. Empty tubes of two different diameters (16 and 25 mm) deformed in diamond mode, while foam filling changed the deformation mode into concertina in 25 mm tube due to thickening effect of foam filling. The strengthening coefficient in concertina mode was found around unity, while in diamond mode it was greater than unity. In concertina mode, foam and tube were observed to deform independently. However, in diamond mode, foam was compressed in between the folds, leading to a higher strengthening coefficient. The effects of deformation rate and the use adhesive on the average crushing loads of the filled tubes were also determined.

© 2004 Elsevier Ltd. All rights reserved.

Keywords: Strengthening coefficient; Axial crushing; Circular aluminum tubes; Foam filling

1. Introduction

The crushing behavior of columnar structures including square and circular metal tubes was studied extensively over the 30 years and has been overviewed by Alghamdi [1]. These structures deform under compression nearly at a constant load, resulting in relatively high-energy absorption efficiency. The studies on foam filled aluminum and steel tubes have also shown that there exists an *interaction effect* between tube wall

* Corresponding author. Tel.: +90 232 4986595, fax: +90 232 4986505.

E-mail address: mustafaguden@iyte.edu.tr (M. Güden).

and foam filler [2–7]. The crushing loads of foam filled tubes are therefore generally found to be higher than the sum of the crushing loads of foam (alone) and tube (alone) mainly due to this effect.

Crushing behavior of aluminum honeycomb and foam filled box columns was numerically and experimentally investigated by Sanatosa and Wierzbicki [7]. It was shown that the effect of filling on the tube crushing load was similar when the strong axis of the honeycomb through and normal to the compression axis, proving that both axial and lateral strength of the filler were effective in increasing the crushing load of the tube. Hannsen et al. [3,5] studied static and dynamic crushing behavior of aluminum foam filled square and circular aluminum extrusions. It was shown that foam filling resulted in a higher number of deformation folds than empty tubes in both static and dynamic tests. This was explained as the stiffness effect of aluminum foam on the sidewalls of the tubes, which decreased the buckling length of the sidewalls. They also developed an equation for the average crushing load (P_{af}) of foam filled columns by including contributions of the average crushing load of empty tube (P_{ae}), foam plateau stress (σ_{pl}) and interaction effect. The equation was found to be well agreed with experimental results and is given as

$$P_{af} = P_{ae} + \sigma_{pl}b^2 + C_{avg}\sqrt{\sigma_{pl}\sigma_o}bt \quad (1)$$

where C_{avg} , σ_o , b and t are the dimensionless constant which is directly related to the interaction effect, yield strength of the tube material and tube width and thickness, respectively. The second term of the right hand side of the Eq. (1) accounts for the axial compression of the foam and the last term for the interaction effect. Santosa et al.[8], based on FEM results, proposed the following equation for the average crushing load of foam filled square tubes of length b ,

$$P_{af} = P_{ae} + C\sigma_{pl}b^2 \quad (2)$$

The constant C in Eq. (2) is considered to be the *strengthening coefficient* of the foam filling. The study of Santosa et al. has also shown that the use of adhesive, although resulting in a relatively small increase in the total weight of the tube, <16%, raised the crushing load of the tube by as much as the foam crushing load.

Many studies on the crushing behavior of the filled tubes were aimed at determining the effect of foam filling on the average crushing load and the specific absorbed energy [2,3,6,9–11] and no systematic study has been performed on the strengthening coefficient of foam filling in circular tubes. In designing with foam filled tubes, knowledge of upper and lower limits of the strengthening is necessary for the calculation of the specific absorbed energy for any tube foam combination. This study was therefore conducted in order to determine the strengthening effect of foam filling in circular thin walled tubes folding with two common modes of deformation: progressive asymmetric (diamond) and progressive axisymmetric (concertina).

Commercially available polystyrene foam was chosen for the filling of the Al tubes with two different tube wall thicknesses and tube diameters. The effects of foam density, deformation rate and the use of adhesive on the average crushing load of the tubes were also determined. Based on experimental results two modes of filler deformation were proposed for the foam filled thin walled tubes.

2. Materials and testing methods

As-received extruded polystyrene foam sheets with dimensions of $5 \times 60 \times 120$ cm were manufactured by IZOCAM Company of Turkey using a process, which produces partly oriented closed-cell foams with smooth continuous skins. The foam sheets investigated were supplied in three different densities with the trade name given to each as: (i) Foamboard[®] 1500, (ii) Foamboard[®] 2500 and (iii) Foamboard[®] 3500. The densities of the foams, hereafter coded as F1500, F2500 and F3500, were determined by dividing the mass of the cubic foam sample ($5 \times 5 \times 5$ cm) by its volume and found to be 21.7 ± 1 , 27.8 ± 2 and 32.1 ± 2 kg m⁻³ for F1500, F2500 and F3500, respectively. The corresponding mean relative densities, 0.0207, 0.0265 and 0.0305, were calculated by dividing the foam density by the dense polystyrene density (1050 kg m⁻³). The cell distribution in each as-received foam sheet was examined through three different planes; Extrusion-Width (E-W), Rise-Width (R-W) and Extrusion-Rise (E-R) as shown in Fig. 1(a). Resulting from foaming process, the cells were preferentially elongated through the thickness or rise direction of the as-received foam sheets (Fig. 1(b)). This gives rise to anisotropy in compression behavior between through rise (R), width (W) and extrusion (E) directions.

The filler crushing behavior was determined by compression testing of cubic samples ($5 \times 5 \times 5$ cm) prepared in accordance with ASTM D1621-91. Compression tests were conducted through R direction with cross-head speeds of 2.5, 8, 25 and 100 mm min⁻¹, corresponding to the strain rates of 8.33×10^{-4} , 2.66×10^{-3} , 8.33×10^{-3} and 3.33×10^{-2} s⁻¹. Compression tests at 8.33×10^{-4} , 8.33×10^{-3} and 1.66×10^{-1} s⁻¹ were also conducted through W and E directions in order to determine the effect cell anisotropy on the compression behavior of the foams.

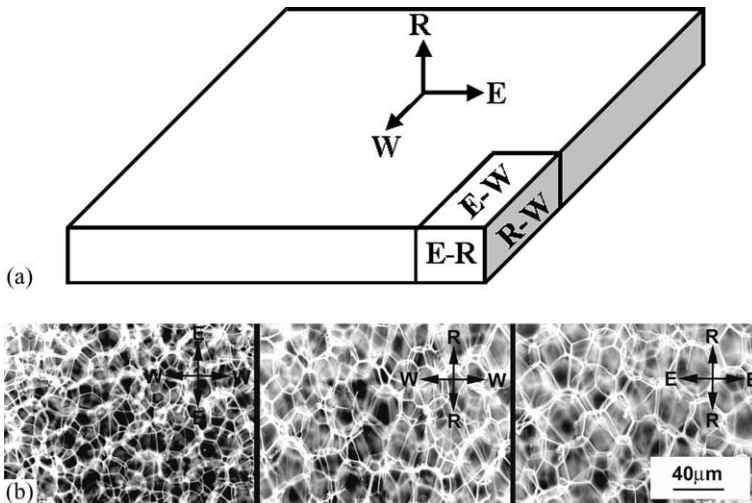


Fig. 1. (a) Schematic of the directions and the planes in as-received foam sheet and (b) transmitted optical micrographs of the cell structure in F2500 through E-W, R-W and E-R planes.

Deep-drawn thin Al tubes (99.7% Al) were produced by METALUM Company of Turkey and received in two different diameters (16 and 25 mm). The thicknesses of the tubes were 0.22 and 0.29 mm for 16 and 25 mm tubes, respectively. The selection of the tube geometries was not arbitrary; empty tubes deformed in diamond, while foam filled 25 mm diameter tube deformed in concertina and foam filled 16 mm diameter tube in diamond mode. Therefore, the strengthening coefficient of foam filling in both modes could be analyzed. The yield and ultimate strength of the tube material was determined by uniaxial tensile tests (ASTM B557M) conducted at a cross-head speed of 2.5 mm min^{-1} and found to be 100 ± 10 and 175 ± 15 MPa, respectively.

Foam filling was through the *R* direction and the skin layer of the filler, which was about 5 mm thick on each faces, was removed. Therefore, the length of empty tubes was chosen 40 mm, same as with that of the filler. The outer diameter of the core-drilled foam inserts was approximately equal to the inner diameter of the tubes; therefore, they were tightly fitted into the tubes. Before foam filling, tubes were kept inside the acetone bath to clean the surfaces. A Bison Styrabond[®] polystyrene adhesive was used to bind the foam filler to the tube wall. The adhesive was first spread on the tube wall and then the foam filler was inserted. The excess adhesive after filler insertion was removed. Filled tubes with adhesive were kept 48 h at room temperature before they were compressed. Compression tests were also conducted without adhesive in order to determine the effect of the adhesive.

Empty and foam filled tubes were compressed at four different cross-head speeds; 2.5, 8, 25 and 100 mm min^{-1} . The corresponding deformation rates, which was defined as the cross-head speed divided by the initial length of the tube, were 1×10^{-4} , 3.33×10^{-3} , 1×10^{-2} and $4.16 \times 10^{-1} \text{ s}^{-1}$. Compressed empty and foam filled tubes until various lengths were cut and then materiallograpically prepared in order to identify the deformation modes.

Tests were conducted using a displacement controlled SHIMADZU AG-I universal testing machine. The average crushing load (P_a) was calculated using following relation:

$$P_a = \frac{\int P d\delta}{\delta} \quad (3)$$

where P and δ are the load and the displacement, respectively. The weights of the tubes and foams were measured before and after foam filling; hence, the weight of the adhesive was calculated and found to be in between 3 and 6% of the total weight of the filled tube.

3. Compression behavior of the Polystyrene foam filler

Fig. 2(a) and (b) show the compression nominal stress-strain curves of the foams tested through *R*, *W* and *E* directions for F1500 and F3500, respectively. Although, compression behavior through *E* and *W* directions are very similar for each density, the foam shows higher compressive stresses in the *R* direction. The difference in the compressive stress between *R* and *W* or *E* directions is also noted to increase with increasing foam density, but decreases with increasing strain. As the foam density increases, the foam compressive

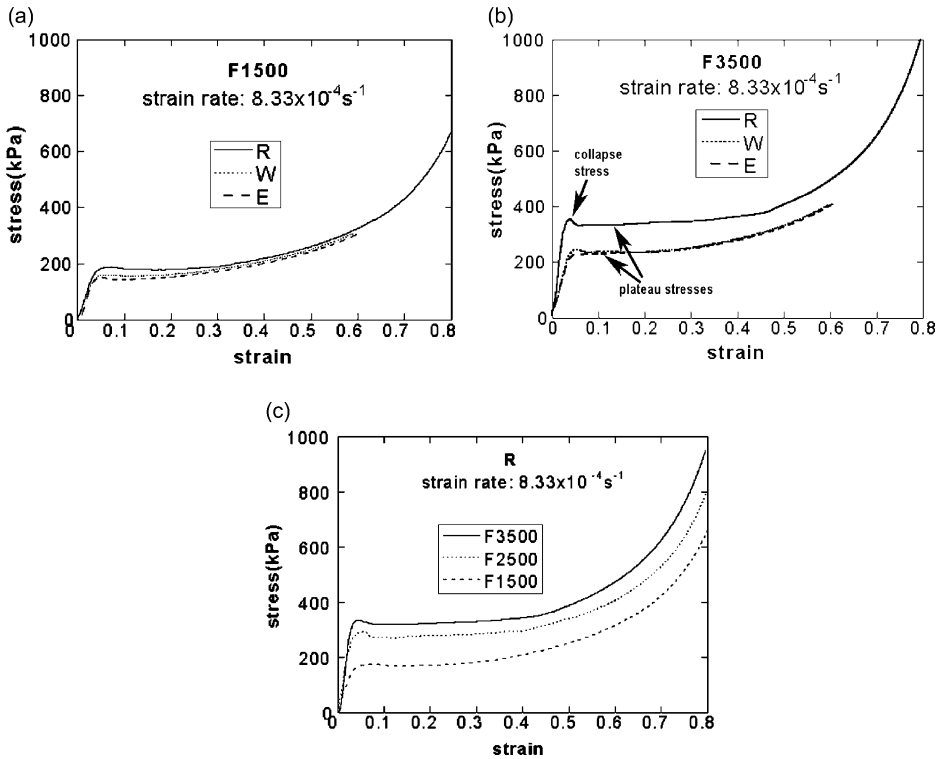


Fig. 2. Nominal compressive stress-strain curves of the foams showing the effect of compression direction in (a) F1500 and (b) F3500 and (c) the effect foam density in the *R* direction.

stress increases for three directions, as shown in Fig. 2(c) for the *R* direction. In all tested foam samples the collapse stress is followed by a plateau region ranging between 0.05 and 0.3–0.4 strains (Fig. 2(b)). At larger strains, >0.3, foam densifies and stress increases significantly over the plateau stress.

The studied foam compressive stress–strain curves are strain rate sensitive and shown in Fig. 3(a) for F2500 at various quasi-static strain rates. The strain rate sensitivity of the foams was further confirmed by the strain rate jump tests, in which the strain rate was suddenly increased or decreased during the test in the plateau and densification region; see Fig. 3(b).

The variation of the plateau stress (Fig. 2(b)) at $8.33 \times 10^{-4} \text{ s}^{-1}$ with foam relative density in *R*, *W* and *E* directions and strain rate in *R* direction is shown in Fig. 4(a) and (b), respectively. The data in Fig. 4(a) were fitted with following power-law strengthening relation,

$$\sigma = K\rho^n \tag{4}$$

where σ and ρ are the stress and foam relative density, respectively and K and n are the constants. It is noted that the value of the n in the *R* direction (~ 1.6) is greater than those in *W* and *E* directions (~ 1 and ~ 1.2), showing a more pronounced density dependence of

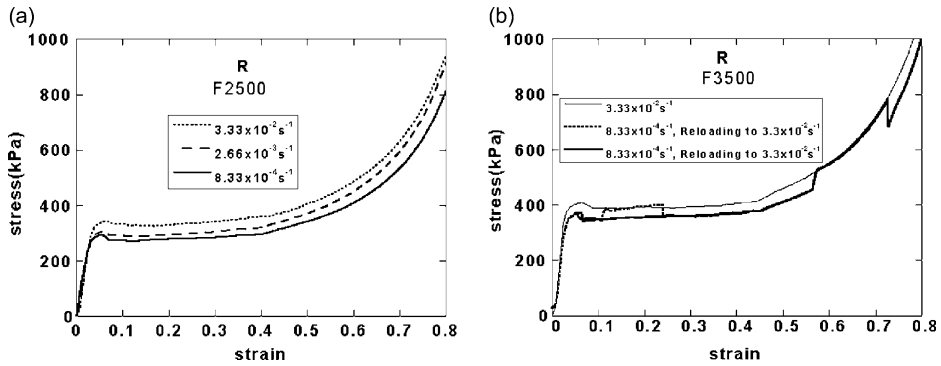


Fig. 3. (a) Effect of strain on the stress-strain curve of the F2500 and (b) strain rate jump test in F3500.

the plateau stress in the *R* direction. The strain rate sensitivity of the foams was found by fitting the plateau stress data in Fig. 4(b) with the following power-law rate strengthening equation

$$\sigma(\dot{\epsilon}) = \sigma_0 \dot{\epsilon}^m \tag{5}$$

where σ_0 , *m* and $\dot{\epsilon}$ are the stress at reference strain rate (1 s^{-1}), the strain rate sensitivity and strain rate, respectively. The strain rate sensitivity parameter of the foam within the studies quasi-static strain rate regime is found to be independent of the foam density and the testing direction and nearly equals to the 0.04 (Fig. 4(b)).

The elastic-plastic foam stress-strain behavior is usually fitted with the gas-pressure hardening equation [12],

$$\sigma = \sigma_c + \frac{P_0 \epsilon}{1 - \epsilon - \rho^*} \tag{6}$$

where σ_c is the initial collapse stress (Fig. 2(b)) and P_0 is the initial gas pressure of the foam cells. In all foam samples tested, the compressive stress versus gas pressure strain ratio ($\epsilon/1 - \epsilon - \rho^*$) curves show two linear regions (after linear elastic region) but with

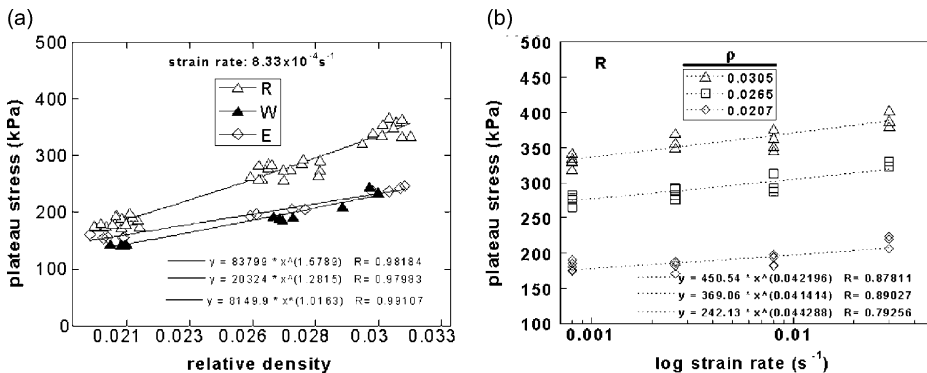


Fig. 4. Plateau stress vs. (a) relative density and (b) strain rate.

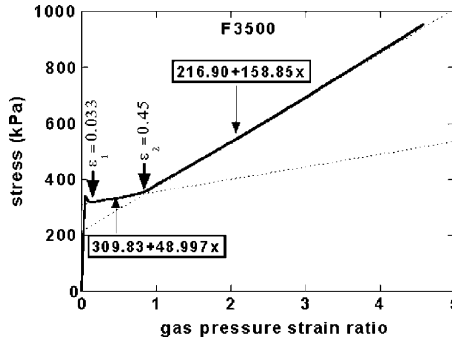


Fig. 5. Stress vs. gas pressure strain ratio of F3500 at $8.33 \times 10^{-4} \text{ s}^{-1}$.

different slopes as shown in Fig. 5 for F3500 tested through *R* direction. In the first linear region the slope is lower than 100 kPa (initial air pressure); while in the second region it is higher than the initial air pressure. Since a linear relationship between stress and gas pressure strain ratio existed, the stress-strain curve corresponding to the lowest strain rate ($8.33 \times 10^{-4} \text{ s}^{-1}$) were fitted with the following equations corresponding region 1, 2 and 3:

$$\sigma = E\varepsilon \quad 0 < \varepsilon < \varepsilon_1 \tag{7}$$

$$\sigma = \sigma_{c1} + S_1 \frac{\varepsilon}{1 - \varepsilon - \rho^*} \quad \varepsilon_1 < \varepsilon < \varepsilon_2 \tag{8}$$

$$\sigma = \sigma_{c2} + S_2 \frac{\varepsilon}{1 - \varepsilon - \rho^*} \quad \varepsilon_2 < \varepsilon < 0.85 \tag{9}$$

where S_1 and S_2 are the slopes of the linear curves in region 2 and 3, respectively. Eq. (7) is for the elastic response of the foam. The parameters of the Eqs. (7)–(9) were first determined for the compression stress-curve at the lowest strain rate ($8.33 \times 10^{-4} \text{ s}^{-1}$) and then using Eq. (5), the parameters were determined for the reference unit strain rate. The parameters of the Eqs. (7)–(9) for the reference strain rate are tabulated in Table 1 for the *R* direction and also determined for the *W* and *E* directions. The stress–strain curves of the foams were then predicted at any strain rate interested within the studied strain rate regime. Fig. 6 shows the predicted stress-strain curves of the F3500 and F1500 foams in the *R* direction at various strain rates.

Table 1
Parameters of Eqs. (7)–(9) at reference strain rate of 1 s^{-1} for the foam tested through *R* direction

Foam	ε_1	ε_2	E (kPa)	σ_{c1} (kPa)	σ_{c2} (kPa)	S_1 (kPa)	S_2 (kPa)	σ_o (at 10% strain) (kPa)	N
F1500	0.033	0.30	7790	254.83	203.69	69.332	188.79	266.18	0.0443
F2500	0.033	0.41	10925	358.03	271.23	56.276	173.79	369.06	0.0414
F3500	0.033	0.45	12791	417.90	292.56	66.051	214.26	450.54	0.0422

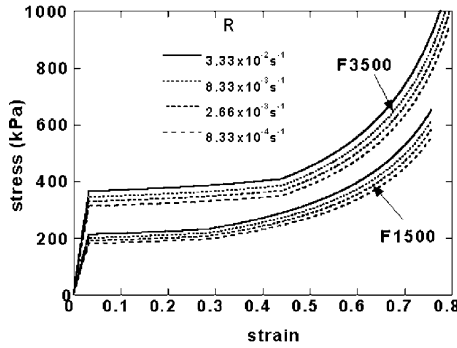


Fig. 6. Predicted stress-strain curves of F3500 and F1500 at various strain rates.

4. Compression behavior of the empty and foam filled tubes

Typical load-displacement curves of the 16 and 25 mm Al empty and foam filled tubes at $1 \times 10^{-4} \text{ s}^{-1}$ are shown in Fig. 7(a) and (b), respectively. Empty tubes deformed in diamond mode. The total number of the folds formed was 9–10 and 7–8 in 16 and 25 mm diameter tubes, respectively. The densification of empty tubes started after 32 mm displacement, corresponding to about 80% of the initial tube length. The top and bottom views of the partially crushed 16 mm tube sample are shown in Fig. 8(a) and (b), respectively. The folds are six-cornered as marked with numbers in Fig. 8(a). Although the first fold formation in empty 25 mm tube was axisymmetric, the deformation proceeded in diamond mode with 8 corners per fold (Fig. 9(a) and (b)). A similar deformation behavior was also previously observed in empty Al tubes and it was due to the influence of the axisymmetric trigger on the first fold [3]. Few of the 25 mm tube samples also deformed in mixed mode. In these samples the first couple of the folds formed in axisymmetric mode then the deformation was turned into diamond mode.

The deformation mode of the foam filled 16 mm Al tube remained to be the same with that of the empty tube. Foam filling however increased load values, reduced the fold length and hence increased the number of folds formed and resulted in shifting of

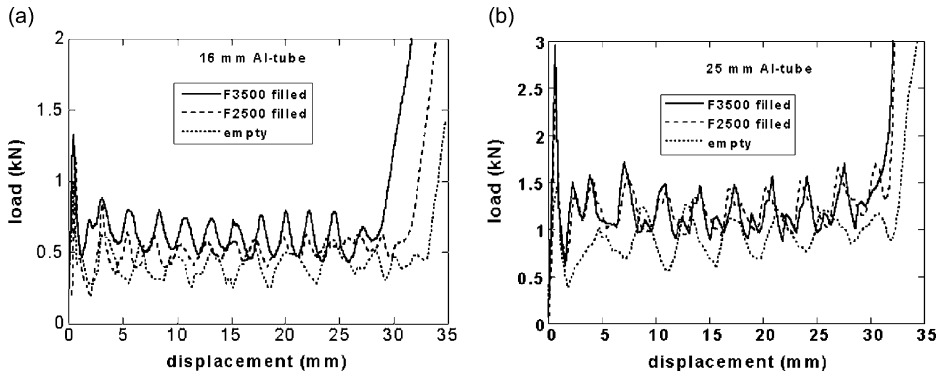


Fig. 7. Typical load vs. displacement curves of the empty and filled tubes (a) 16 and (b) 25 mm tubes.

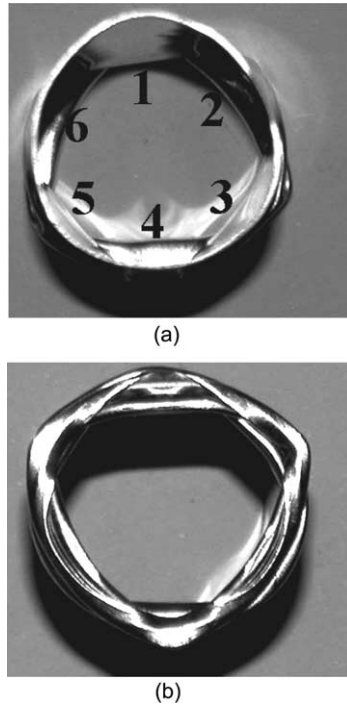


Fig. 8. Views of the partially compressed 16 mm empty tube, (a) top and (b) bottom.

the densification point to lower values of the displacement (Fig. 7(a)). The effect of increasing foam density was to increase the load values and lower the densification point (Fig. 7(a)). In these filled tubes, the first fold usually formed in axisymmetric mode, but the deformation proceeded in diamond mode and totally 10–12 folds formed regardless of the foam density (Fig. 10(a)). It is also noted that the elastic recovery of the foam-filler was prevented by the tube wall due to the entrance of the foam in between the folds (Fig. 10(b)).

For the studied foam densities, the foam filling of 25 mm Al tube resulted in change of deformation from diamond into concertina mode; see Fig. 11 (a) and (b). Few of the F1500 foam filled tube samples also deformed in mixed mode. In concertina mode of deformation the foam filler partly recovered elastically after unloading; part of the foam remained to be attached to crushed tube wall and that resulted in tearing of the filler (Fig. 11(a)). The effect of foam filling on the load-displacement behavior of the 25 mm Al tube, as in the case of 16 mm tube, was to increase of the load values, reduce fold length and hence increase number folds and lower the densification point (Fig. 7(b)). Increasing foam density increased the load values but also slightly lowered the densification point (Fig. 7(b)).

The effect of deformation rate on the load-displacement curves of the empty and foam filled tubes are shown in Fig. 12(a–d) for 16 mm tube. There is a slight or negligible effect of deformation rate on the load-displacement behavior of the empty tubes. In foam filled 16 mm tube, the increasing deformation rate increases the load values (Fig. 12(b–d)),

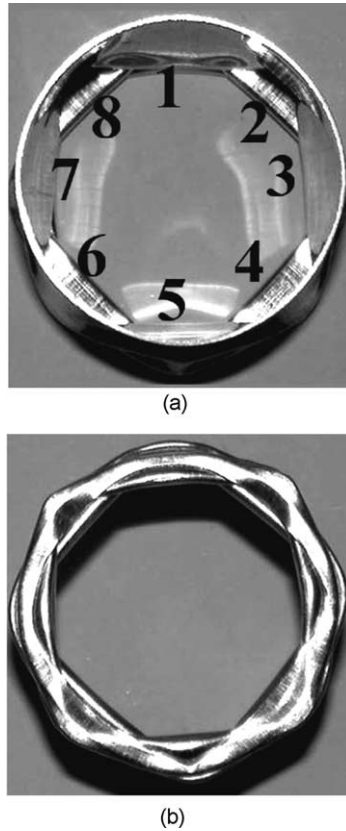


Fig. 9. Views of the partially compressed 25 mm empty tube, (a) top and (b) bottom.

mostly arising because of the strain rate dependent compressive flow stress of the foam. A similar effect of deformation rate on the load-displacement behavior of the 25 mm empty and foam filled Al tubes was also found.

The average crushing load values of the empty and foam filled tubes showed a maximum initially and then reached almost a constant value as the displacement increased

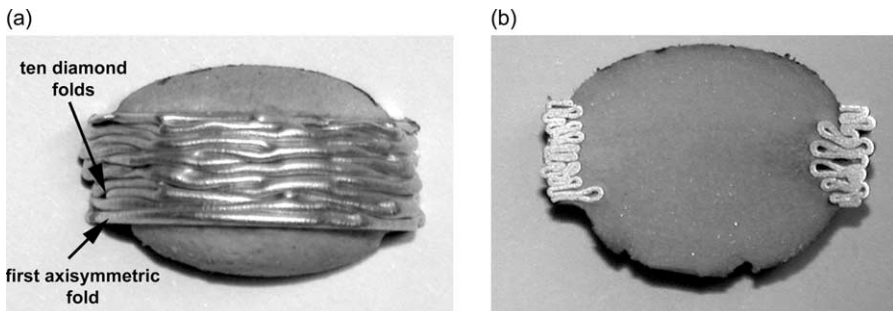


Fig. 10. (a) Side view of F1500 filled and (b) interior view of F3500 filled compressed 16 mm tubes.

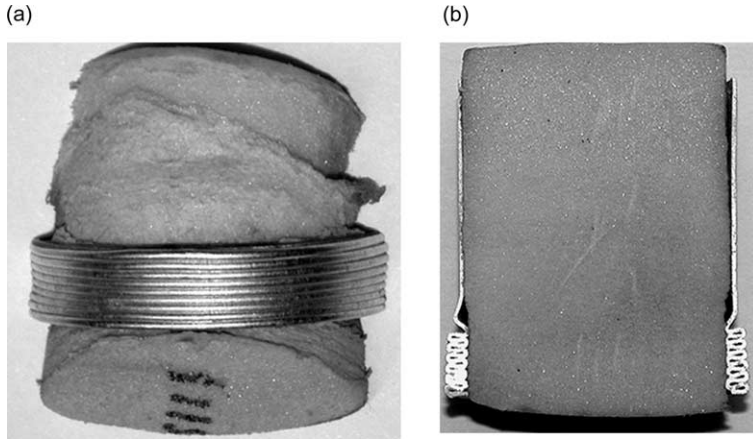


Fig. 11. F3500 filled 25 mm Al tube views, (a) side and (b) interior (partially compressed).

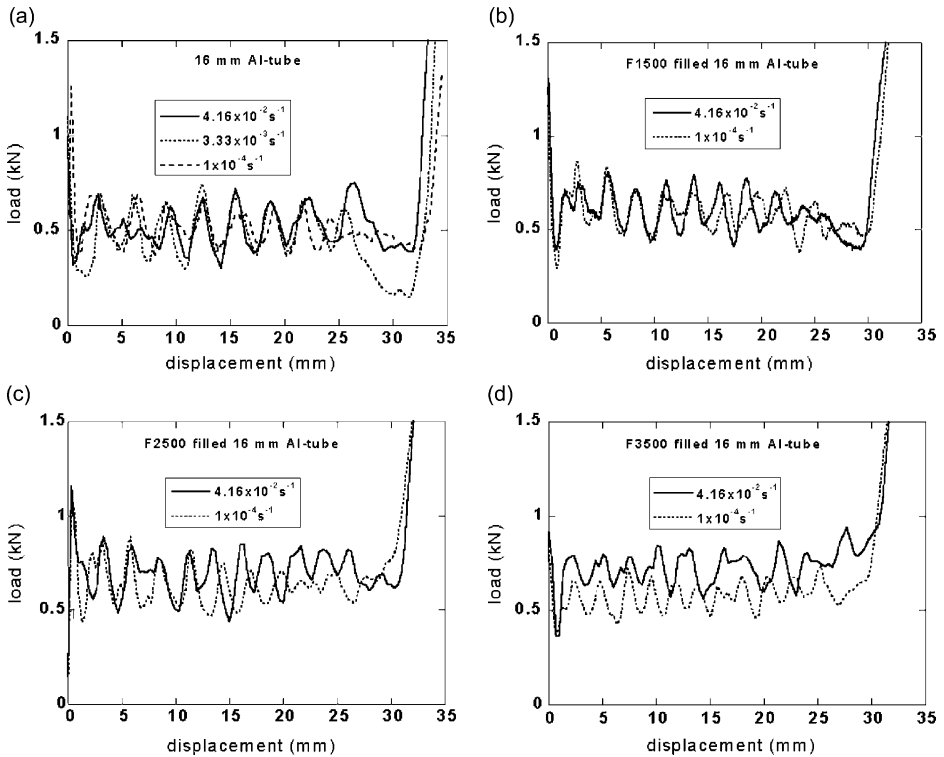


Fig. 12. Effect of deformation rate on the load-displacement curves; (a) empty (b) F1500, (c) F2500 and (d) F3500 filled 16 mm Al tubes.

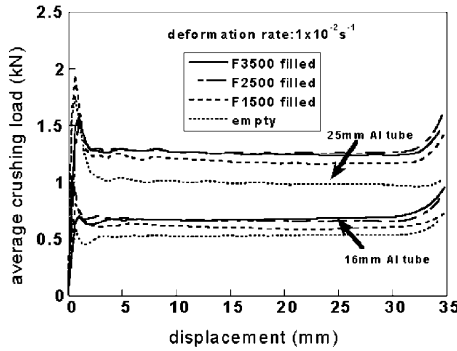


Fig. 13. Effect of foam filling on the average crushing load of the 16 and 25 mm tubes at $1 \times 10^{-2} \text{ s}^{-1}$.

(Fig. 13). The effect of deformation rate on the average crushing load of the empty and filled tubes at 50% deformation is shown in Fig. 14. The deformation rate increases the average crushing loads of the filled tubes. Each datum given in these figures is the average values of the at least three tests.

The use of adhesive in 16 mm Al foam filled tubes increased the average crushing loads slightly especially at low displacements; however, no significant effect of the adhesive was found in foam filled 25 mm Al tube (Fig.15 (a) and (b)).

5. Strengthening effect of foam filling

The simplest approach for predicting average crushing load of foam filled tubes is to add the foam crushing load, which is usually taken as the load corresponding to the plateau stress, to the empty tube average crushing load. In this approach, the foam filler and tube are assumed to deform independently. This approach generally gives the average crushing load values lower than experimental values due to the interaction effect between tube wall and filler. The interaction effect was also found in the tested polystyrene foam filled Al tubes (Fig. 16).

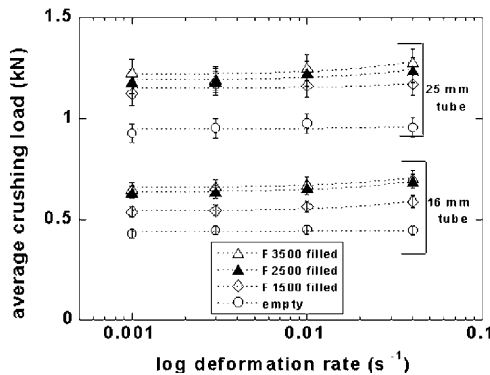


Fig. 14. Average crushing load vs. deformation rate.

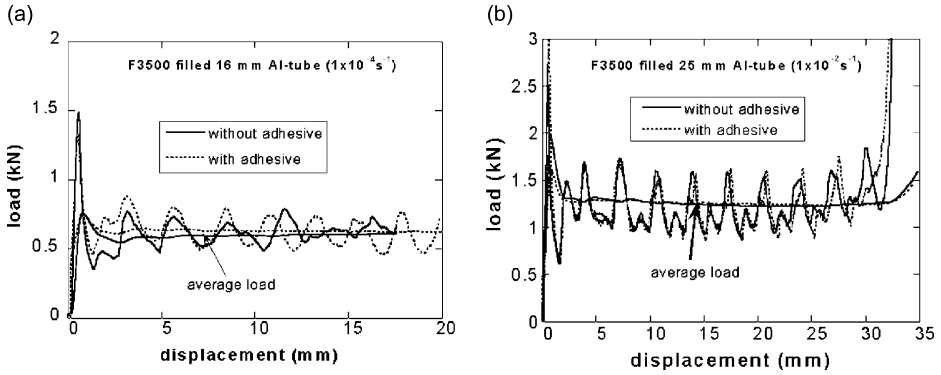


Fig. 15. Effect adhesive on the load and average crushing load values of (a) 16 and (b) 25 mm filled tubes.

Rearranging Eq. 2 for the circular tube gives the C as

$$C = \frac{P_{af} - P_{ae}}{\sigma_{pl}\pi R^2} = \frac{\Delta P_a}{P_{foam}} \tag{10}$$

where P_{foam} is the foam load corresponding to the plateau stress. For the present foam filled tubes, two different foam loads were used to calculate strengthening coefficient: loads corresponding to the plateau stress in the R direction and the sum of the plateau stresses in the R and W directions. The results are shown in Fig. 17(a) and (b) for foam load of R and $R + W$ directions, respectively. Note also the slopes of the curves in Figs. 17(a) and (b) correspond to the strengthening coefficient given in Eq. (10). For the foam load of R direction, the increase in the filled tube crushing load is about 3.2 times of the foam load for 16 mm tube, while a smaller strengthening coefficient is found for 25 mm tube, 1.82. For the foam load of $R + W$, the strengthening coefficients are about 1.8 and 1 for 16 and 25 mm tubes, respectively.

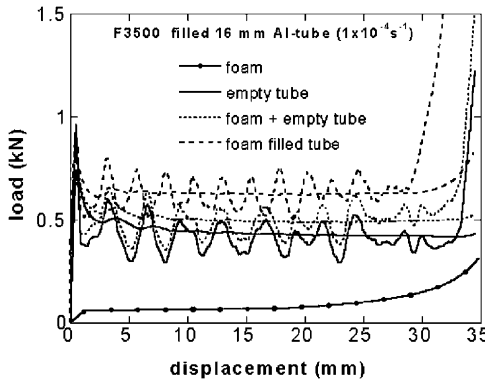


Fig. 16. The interaction effect in 16 mm Al tube; filled tube shows higher average crushing load than that of foam+empty tube.

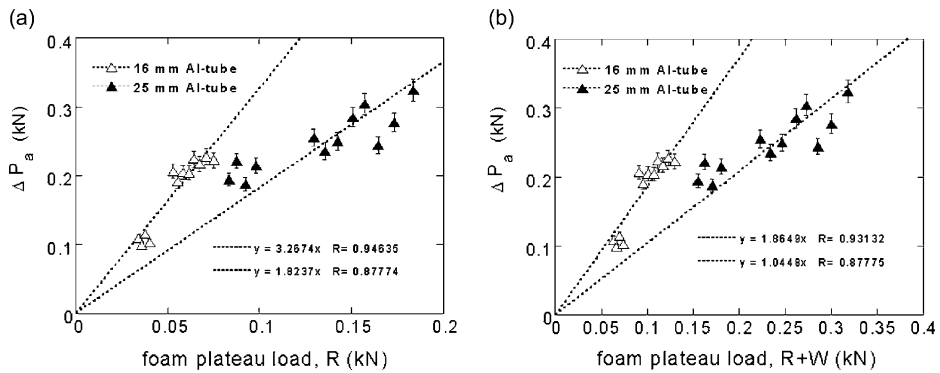


Fig. 17. ΔP_a vs. foam plateau load; (a) R and (b) $R+W$.

In the filled tubes, the interaction effect may be partly due to the resistance of the filler to the inward and/or outward folding of the tube and partly due to the interfacial friction stress between foam and tube wall. Numerical studies of Al foam and honeycomb filled tubes have shown a negligible effect of interfacial frictional stress on the crushing strength of tubes [7,8]. In order to validate this assumption, foam samples were compressed in 25 mm Al tube (confinement test) and the resulting load-displacement curves were compared with those of the compression tested samples (5 cm cube). A similar load-displacement behavior was found, except the load values of the confinement test in the densification region were slightly lower, proving a negligible effect of interfacial stress. The strengthening coefficients of Al foam filled square tubes with and without adhesive were numerically and experimentally shown to be 1.8–2 and 2.8, respectively [7,8,13]. It was also found that the use of adhesive may change the triggering position of the folding from the end of the tube to the mid sections [2,13]. This is basically due to the effect of local inhomogeneity of the foam which forms a favorable side for the fold formation on the tube. In polystyrene foam filled tubes, folding started at one end of the tube in all tested samples, which proved the relatively homogenous cell size distribution of the foam used.

The deformation cross-sections of the 16 mm foam filled tubes with and without adhesive are shown in Figs. 18 (a–c). It is noted in these figures, the tube and filler deformation started at the end of the tube (shown by arrows) and the filler deformation was localized in the fold region of the tubes of the with and without adhesive (Fig. 18(c)).

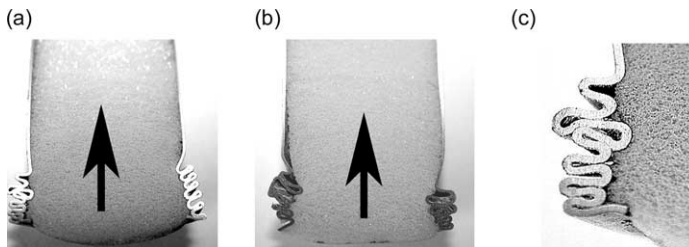


Fig. 18. Cross-sections of the partially compressed F3500 filled 16 mm tube, (a) with adhesive, (b) without adhesive and (c) magnified with adhesive.

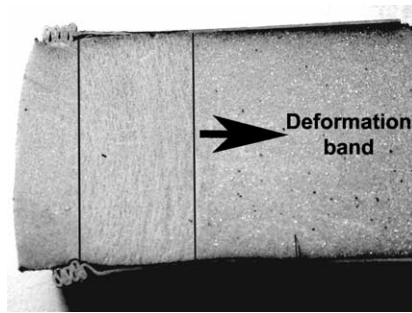


Fig. 19. Partially compressed F3500 filled 25 mm Al tube.

Close inspection of the 25 mm foam filled tubes cross-sections showed that, foam and tube deformed independently in most part of deformation (Fig. 19). In the filled tubes with adhesive, it was observed that the filler peeled off completely and/or partially from the tube wall after the first fold; therefore, the use of adhesive became ineffective. Mainly due to this effect, the load-displacement curves of the filled tubes with and without adhesive were found to be the same.

Since the foam deformation started in and proceeded within the fold region in 16 mm Al tube, the local strain of the filler in the crushed region may be assumed to scale with the fold length. The fold length can be roughly calculated using the following relation:

$$H_f = \frac{DP \times L}{N} \quad (11)$$

where H_f , DP , L and N are the fold length of foam filling, densification strain (~ 0.75), the initial length of the filled tube (40 mm) and the total number of folds formed, respectively. About 11 folds were formed in the foam filled 16 mm tube, corresponding to the fold length of 2.73 mm. Assuming the folds moved until the faces of the folds touches to each other, the strain of the foam in the fold region will be

$$\varepsilon_f = \frac{H_f - 2t}{H_f} \quad (12)$$

where t is the thickness of the tube. Eq. (12) gives a compression strain of the filler about 0.75. Replacing foam R load with the load corresponding 0.75 strain for the 16 mm tube gives a strengthening coefficient of 1 for the tested foam filled samples (see Fig. 20).

The strengthening coefficient of the polystyrene foam filling of the present study was also compared with those of the previous experimental studies on Al and polyurethane foam filled Al circular tubes [3,6,14]. The comparison is shown in Fig. 21, in which the strengthening coefficient is plotted as function of foam/empty tube load ratio. Three distinct regions designated as 1, 2 and 3, are shown in this figure. In region 1, foam filling does not change the deformation mode: both empty and filled tubes deform in diamond or mixed mode. As the foam load increases, the deformation changes into mixed or concertina mode and in the third region, it is predominantly concertina. The highest strengthening coefficients, ranging between 2 and 4, are found in Region 1, where the foam load is relatively low as compared with the tube crushing load and foam filling does not

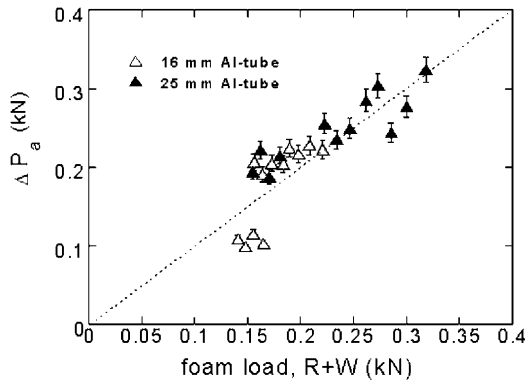


Fig. 20. ΔP_a vs. foam plateau load in the $R+W$ directions, rearranged for the load corresponding 0.75 strain in the R direction for 16 mm tube.

change the deformation mode. In region 2, the foam filling switches deformation mode from diamond into mixed or concertina and the strengthening coefficient in this region fluctuates around 2. In the last region, the deformation mode is predominantly concertina and the strengthening coefficient is below 2 but still higher than 1. The polystyrene foam filling of the present study shows good agreements with previous studies. For 16 mm tubes, in which the empty and foam filled tubes deform in diamond mode, the strengthening coefficients ranges between 2.7–4.5. The strengthening coefficient of the foam filled 25 mm tubes, in which the deformation mode shifted to concertina is around 2. The present results are also well accord with the experiemental and numerical results of Santosa et al. [8] in the case of without adhesive.

Based on experimental results and microscopic observation of crushed cross-sections, two modes of deformation of the polystyrene foam filled thin-walled Al tubes are proposed. The first mode features the axial deformation of the foam filler in between the folds or in the fold region. In this mode, tube folding and filler axial deformation occur

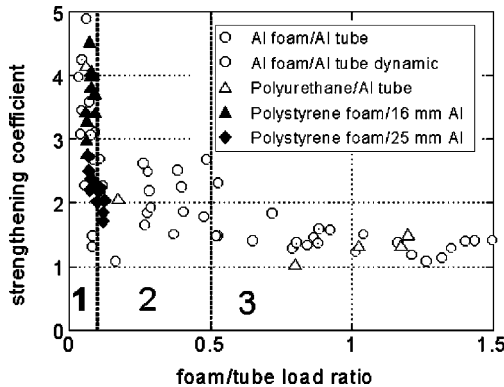


Fig. 21. Comparison of the experimentally determined strengthening coefficients with those of the previous studies on foam filled circular tubes.

together in the same region. Therefore, the foam deformation is determined by the amount of axial deformation of the fold length and may be well above the critical strain for densification; hence the foam load may be above the load of plateau stress. This model corresponds to the diamond mode of deformation of the polystyrene foam filled 16 mm tubes in this study. The second mode is based on the independent deformation of the tube and filler. Therefore, the localized deformation of the foam and tube occur in different regions.

6. Conclusions

The strengthening effect of foam filling in thin-walled tubes was investigated in polystyrene foam filled Al tubes in two modes of deformation. The foam filling was found to change the deformation mode of the 25 mm Al tube from diamond into concertina due to the thickening effect of the foam filling. The effect of foam filling was to increase the average crushing load over that of the tube (alone) + foam (alone), known as interaction effect. In 16 mm Al tube with and without adhesive, the foam deformed in between the folds. In 25 mm Al tube, the adhesive was presumed to be separated from the tube wall at the early stage of the folding, mainly due to the localized deformation of the filler in the mid sections. The deformation of the filler between the folds was likely to exceed the plateau stress of the foam, giving a higher strengthening coefficient in foam filled 16 mm Al tubes as compared with 25 mm Al tubes.

Acknowledgements

The authors would like to thank the IZOCAM and METALUM Company of Turkey for supplying polystyrene foams and Al tubes.

References

- [1] Alghamdi AAA. Collapsible impact energy absorbers: an overview. *Thin-Walled Struct* 2001;39:189–213.
- [2] Seitzberger M, Rammerstorfer FG, Degischer HP, Grandiger R. Crushing of axially compressed steel tubes filled with aluminium foam. *Acta Mech* 1997;125:93–105.
- [3] Hanssen AG, Langseth M, Hopperstad OS. Static and dynamic crushing of circular aluminium foam filler. *Int J Impact Eng* 2000;24:475–507.
- [4] Seitzberger M, Rammerstorfer FG, Gardinger R, Degischer HP, Blaimschein M, Walch C. Experimental studies on the quasi-static axial crushing of steel columns filled with aluminium foam. *Int J Solids Struct* 2000;37:4125–47.
- [5] Hanssen AG, Langseth M, Hopperstad OS. Static and dynamic crushing of square aluminium extrusions with aluminium foam filler. *Int J Impact Eng* 2000;24:347–83.
- [6] Guillow SR, Lu G, Grezbieta RH. Quasi-static axial compression of thin-walled circular aluminium tubes. *Int J Mech Sci* 2001;43:2103–23.
- [7] Santosa SP, Wierzbicki T. Crash behavior of box columns filled with aluminum honeycomb or foam. *Comput Struct* 1998;68:343–67.

- [8] Santosa SP, Wierzbicki T, Hanssen AG, Langseth M. Experimental and numerical studies of foam-filled sections. *Int J Impact Eng* 2000;24:509–34.
- [9] Singace AA. Collapse behaviour of plastic tubes filled with wood sawdust. *Thin-Walled Struct* 2000;37:163–87.
- [10] Hanssen AG, Langseth M, Hopperstad. Optimum design for energy absorption of square aluminium columns with aluminium foam filler. *Int J Mech Sci* 2001;43:153–76.
- [11] Hall IW, Ebil O, Guden M, Yu CJ. Quasi-static and dynamic crushing of empty and foam filled tubes. *J Mater Sci* 2001;36:5853–60.
- [12] Gilchrist A, Mills NJ. Impact deformation of rigid polymeric foams: experiments and FEA modeling. *Int J Impact Eng* 2001;25:767–86.
- [13] Toksoy AK, Tanoglu M, Guden M, Hall I. The effect of adhesive on the strengthening of aluminum foam-filled circular tubes. *J Mater Sci Lett*. 2004;39:1503–6.
- [14] Ku JH, Seo KS, Park SW, Kim YJ. Axial crushing behavior of the intermittent tack-welded cylindrical tubes. *Int J Mech Sci* 2001;43:521–42.